

Spatiotemporal models for Poisson areal data with an application to the AIDS epidemic in Rio de Janeiro

Marco A. R. Ferreira¹, Juan C. Vivar²

Abstract

We present a class of spatiotemporal models for Poisson areal data suitable for the analysis of emerging infectious diseases. These models assume Poisson observations related through a link equation to a latent random field process. This latent random field process evolves through time with proper Gaussian Markov random field convolutions. Our approach naturally accommodates flexible structures such as distinct but interacting temporal trends for each region and across-time contamination among neighboring regions. We develop a Bayesian analysis approach with a simulation-based procedure: specifically, we construct a Markov chain Monte Carlo algorithm based on the generalized extended Kalman filter to obtain samples from an approximate posterior distribution. Finally, for the comparison of Poisson spatiotemporal models, we develop a simulation-based conditional Bayes factor. We illustrate the utility and flexibility of our Poisson spatiotemporal framework with an application to the number of acquired immunodeficiency syndrome (AIDS) cases during the period 1982-2007 in Rio de Janeiro.

Key Words: Bayesian inference; Dynamic generalized linear models; Exponential family data; Regional data; State-space models.

¹(to whom correspondence should be addressed) Department of Statistics, Virginia Tech, 406-A Hutcheson Hall, 250 Drillfield Drive, Blacksburg, VA 24061, marf@vt.edu

²Food and Drug Administration

1 Introduction

There is an increasing need for models for the spatiotemporal spread of emerging infectious diseases. This increasing need arises from several factors such as the impact of global warming on spread of insect vectors (Lafferty, 2009; Epstein, 2010) and higher global mobility of goods and people (Apostolopoulos and Sönmez, 2007). These factors have substantially increased the risk of epidemics of new, emerging, and re-emerging infectious diseases (Brower and Chalk, 2003). In terms of publicly available information, datasets on diseases are usually in the form of areal count data; that is, total number of cases of the disease available in a partition of the geographical domain of interest (Banerjee et al., 2014). These areal count data are usually modeled using the Poisson distribution. Several spatiotemporal models for Poisson areal data have been developed in the disease mapping literature (e.g., Bernardinelli et al., 1995; Waller et al., 1997; Knorr-Held, 2000; Schmid and Held, 2004; Tzala and Best, 2008). Usually, these models assume a common univariate temporal trend for all the regions and time-specific spatial random effects. When modeling non-infectious diseases such as cancer, these models are usually effective to explain the remaining spatiotemporal noise after covariates are taken into account. However, these models are not appropriate for modeling the spatiotemporal dynamics of infectious diseases. In contrast, Vivar and Ferreira (2009) have introduced a general class of linear Gaussian spatiotemporal models for areal data that allows for more complex spatiotemporal processes. Even though the Gaussian model framework of Vivar and Ferreira (2009) may be applied to transformed count data when the counts are large, their framework is inadequate for dealing with counts that are small. Hence, their framework would not be appropriate for modeling the early epidemic expansion stages of an emerging disease. Here we develop methodology that can be directly applied to areal count data. Specifically, we propose a spatiotemporal class of models that allows for more complex spatiotemporal processes for Poisson areal data.

There has been some previous literature where each subregion of the geographical domain of interest may have a different temporal trend (Sun et al., 2000; Assuncao et al., 2001;

MacNab and Dean, 2001). Typically, these models assume time-specific spatial random effects that follow a Gaussian Markov random field. Furthermore, they assume region-specific temporal trends that are deterministic functions of time and may be linear (Sun et al., 2000), quadratic (Assuncao et al., 2001), or piecewise cubic (MacNab and Dean, 2001). Finally, Sun et al. (2000), Assuncao et al. (2001), and MacNab and Dean (2001) assume that the temporal trend coefficients follow Gaussian Markov random fields. Even though these previous works allow for similar deterministic temporal trends for neighboring regions, they do not allow for more flexible temporal trends. Conversely, as we detail in Section 2.1, our novel class of models allows for more flexible stochastic temporal trends and for spatiotemporal interaction among the different regions.

There are two main modeling approaches to analyze epidemic data. One of these approaches is through compartmental susceptible/exposed/infectious/ removed (SEIR) models (e.g., see Anderson and May, 1992). Based on the local behavior of individuals, these SEIR models assume that the expected epidemic dynamics in the population can be represented by a set of partial differential equations. Because SEIR models are based on the local behavior of individuals, Mugglin et al. (2002) say that SEIR models provide a “particle” view of the spread of an epidemic. The other modeling approach is what Mugglin et al. (2002) call a “field” view. This field view approach pioneered by Mugglin et al. (2002) is particularly adequate for spatiotemporal areal data and models the stochastic geographic spread of the epidemic through time using a multivariate dynamic generalized linear model. Specifically, Mugglin et al. (2002) model the spatiotemporal dynamics of an influenza epidemic with what they call a spatially descriptive temporally dynamic hierarchical model. Their model is a particular case of our class of models where they use what we call a contamination model. Similarly to Mugglin et al. (2002), here we take a field view of the spatiotemporal epidemic process.

To perform Bayesian statistical analysis for our proposed class of spatiotemporal models, here we develop a simulation-based procedure. Specifically, we construct a Markov

chain Monte Carlo (MCMC) algorithm (Gelfand and Smith, 1990; Robert and Casella, 2004; Gamerman and Lopes, 2006) to obtain samples from an approximate posterior distribution. The MCMC algorithm we propose combines the generalized extended Kalman filter (p. 352, Fahrmeir and Tutz, 2001) and the forward filter backward sampler method (FFBS) (Frühwirth-Schnatter, 1994; Carter and Kohn, 1994) for the simulation of the latent fields. Our computational methodology is general enough to be applied to observations with any distribution in the regular exponential family. However, here we focus on Poisson observations.

With the ability to fit several nonnested spatiotemporal models comes the need to compare those models. In addition, when analyzing a particular dataset, each of the fitted models corresponds to a distinct scientific hypothesis. As such, comparison of the different models becomes paramount for understanding the nature of the process underlying the observed data. For the comparison of the resulting nonnested Poisson spatiotemporal models, we develop a conditional Bayes factor (p. 190, Ghosh et al., 2006) computed by using the output of our MCMC algorithm. As we discuss in Section 3.2, this conditional Bayes factor provides a model comparison criterion that is justified from a Bayesian decision-theoretic point of view (Berger, 1985). In addition, this conditional Bayes factor is computed based on the one-step ahead predictive densities of the competing models. Therefore, as an important practical consequence, this conditional Bayes factor favors models that provide better probabilistic predictions.

We illustrate the utility and flexibility of our Poisson spatiotemporal framework with an application to the number of acquired immunodeficiency syndrome (AIDS) cases in Rio de Janeiro State, Brazil. Specifically, we consider the annual number of cases of AIDS from 1982 to 2007 for each of the 92 counties in Rio de Janeiro State. These data are publicly available from the Ministry of Health of Brazil and may be downloaded from the webpage <https://datasus.saude.gov.br>. AIDS is caused by the immunodeficiency virus (HIV), which has a long incubation period with a median of about 10 years in young adults

(Bacchetti and Moss, 1989). Because the incubation period is much longer than the observational time unit of one year, we may expect the observed number of cases in one year to be a convolution of infections that have occurred in several previous years. As a result, the change from year to year in the underlying latent expected number of cases may have a strong spatial dependence. Finally, given the time scale of the incubation period of about one decade and the fact that AIDS has emerged about four decades ago, the AIDS epidemic provides an excellent case study of what may be the spatiotemporal dynamics when a disease is emerging in a previously unaffected region.

This chapter is organized as follows: Section 2 presents the proposed general class of spatiotemporal Poisson models for epidemic areal data, as well as several useful specific models. Section 3 develops simulation-based Bayesian estimation and model selection for these spatiotemporal models. Section 4 illustrates our spatiotemporal framework with an application to the number of AIDS cases in the State of Rio de Janeiro, Brazil. Conclusions and possible extensions are presented in Section 5.

2 Spatiotemporal Models for Poisson Areal Data

Consider a geographical domain of interest partitioned in a collection of S regions indexed by the integers $1, \dots, S$ forming a regular or irregular grid. Assume that this grid is endowed with a neighborhood system $\{N_s, s = 1, \dots, S\}$, where N_s is the set of regions that are neighbors of region s . Let y_{ts} be the number of cases observed at time t on region s , $t = 1, \dots, T$, $s = 1, \dots, S$. As usual for count data, assume that the observation y_{ts} follows a Poisson distribution. Specifically, assume that $y_{ts} | \lambda_{ts} \sim Po(n_{ts} \lambda_{ts})$, where n_{ts} denotes the population size and λ_{ts} is the underlying risk at time t and region s , $t = 1, \dots, T$, $s = 1, \dots, S$. Thus, the probability function of y_{ts} conditional on λ_{ts} is

$$p(y_{ts} | \lambda_{ts}) = \frac{(n_{ts} \lambda_{ts})^{y_{ts}} e^{-n_{ts} \lambda_{ts}}}{y_{ts}!}. \quad (1)$$

Let $\eta_{ts} = \log(n_{ts}\lambda_{ts})$, $a = 1$, $b(\eta_{ts}) = n_{ts}\lambda_{ts} = \exp(\eta_{ts})$, and $c(y_{ts}) = -\log(y_{ts}!)$. Then, the Poisson probability function can be rewritten as (Casella and Berger, 2001)

$$p(y_{ts}|\eta_{ts}, v) \propto \exp\{(y_{ts}\eta_{ts} - b(\eta_{ts}))/a + c(y_{ts})\}, \quad (2)$$

and thus belongs to the regular exponential family of distributions. Here, the natural parameter is $\eta_{ts} = \log(\mu_{ts})$, where $\mu_{ts} = b'(\eta_{ts}) = \exp(\eta_{ts}) = n_{ts}\lambda_{ts}$ is the mean of y_{ts} . Hence, we may rewrite the natural parameter as $\eta_{ts} = \log n_{ts} + \log \lambda_{ts}$.

To model the mean level, generalized linear models assume a monotone differentiable link function $g(\cdot)$ that transforms the mean μ_{ts} from its restricted range to the unrestricted real line (McCullagh and Nelder, 1989). For example, in the case of Poisson data a typical choice is the canonical link function $g(\mu) = \log \mu$. In the spatiotemporal case we consider, the canonical link function becomes $g(\mu_{ts}) = \log(\mu_{ts}) = \log n_{ts} + \log \lambda_{ts}$, where $\log n_{ts}$ is a known offset. In this case, we define $\theta_{ts} = \log \lambda_{ts}$ as the value of the latent log-risk random field at time t and region s . Then, we may directly relate θ_{ts} to the natural parameter η_{ts} through the function $\delta_{ts}(\cdot)$ defined as

$$\eta_{ts} = \delta_{ts}(\theta_{ts}) = \theta_{ts} + \log n_{ts}. \quad (3)$$

Finally, assuming the canonical link function $g(\mu_{ts}) = \log(\mu_{ts}) = \log n_{ts} + \log \lambda_{ts}$ implies that the so-called response function, i.e. the inverse of the link function, is $f(\theta_{ts}) = n_{ts} \exp(\theta_{ts})$. The response function plays an important role in the construction of the generalized extended forward filter detailed in Algorithm 3.1.

Let $\boldsymbol{\theta}_t = (\theta_{t1}, \dots, \theta_{ts})'$ be the vectorized latent log-risk random field at time t . We relate $\boldsymbol{\theta}_t$ to a dynamic latent vector $\boldsymbol{\beta}_t$ through the linear equation

$$\boldsymbol{\theta}_t = \mathbf{F}_t' \boldsymbol{\beta}_t, \quad (4)$$

where \mathbf{F}_t is typically known up to some few unknown hyperparameters. Finally, we assume that the latent vector $\boldsymbol{\beta}_t$ evolves through time following the system (also known as evolution or state-space) equation

$$\boldsymbol{\beta}_t = \mathbf{G}_t \boldsymbol{\beta}_{t-1} + \boldsymbol{\omega}_t, \quad \boldsymbol{\omega}_t \sim PGMRF(\mathbf{0}, \mathbf{W}_t^{-1}), \quad (5)$$

where the evolution matrix \mathbf{G}_t is usually known up to some few unknown hyperparameters. Equation (5) generalizes the dynamic generalized linear model system equation of West et al. (1985); Prado et al. (2021) to the multivariate spatiotemporal case. Further, $\boldsymbol{\omega}_t$ is a vector of evolution innovations that follows the proper Gaussian Markov random field (PGMRF) process discussed in Section ?? with zero mean vector and precision matrix \mathbf{W}_t^{-1} , that is, the density of $\boldsymbol{\omega}_t$ is proportional to

$$|\mathbf{W}_t|^{-0.5} \exp(-0.5 \boldsymbol{\omega}_t' \mathbf{W}_t^{-1} \boldsymbol{\omega}_t),$$

where the precision matrix is $\mathbf{W}_t^{-1} = \tau(\mathbf{I} + \phi \mathbf{M})$. Here, $\tau > 0$ is a scale parameter, $\phi > 0$ controls the amount of spatial correlation, and \mathbf{I} is the identity matrix. In addition, the neighborhood matrix \mathbf{M} is such that $(\mathbf{M})_{k,l} = m_k$ if $k = l$, $(\mathbf{M})_{k,l} = -g_{kl}$ if $k \in N_l$, and $(\mathbf{M})_{k,l} = 0$ otherwise, where $g_{kl} > 0$ is a measure of similarity between regions k and l , and the diagonal elements are defined as $m_k = \sum_{l \in N_k} g_{kl}$, $k = 1, \dots, S$. For additional details on this type of PGMRFs, see Ferreira and De Oliveira (2007).

2.1 Spatiotemporal Models for Epidemics

This section discusses several important specific models within the general class of models defined by Equations (1), (3), (4), and (5) that are useful for spatiotemporal modeling of epidemics. Epidemic processes of emerging diseases, as is the case of the AIDS data that we consider, are usually nonstationary at the start of the epidemic. Thus, here we consider five distinct nonstationary state-space equation specifications. Further, for each of these five specifications, we consider two distinct state-space covariance matrices, comprising a total of ten models. The first covariance matrix is diagonal, and the second covariance matrix is defined (as discussed above) as the covariance matrix of a PGMRF.

The first state-space equation specification we consider is a first-order temporal trend evolution. Specifically, the first-order temporal trend evolution assumes $\mathbf{F}'_t = \mathbf{I}_S$ and $\mathbf{G}_t = \mathbf{I}_S$. This matrix \mathbf{F}_t implies that β_{ts} is the log of the risk at time t for each person in

subregion s . When the state-space precision matrix is the PGMRF matrix $\mathbf{W}_t^{-1} = \tau(\mathbf{I}_S + \phi\mathbf{M})$, the implied expected value of β_{ts} , $t = 2, \dots, T-1$, conditional on the entire latent process is $0.5(\beta_{t-1,s} + \beta_{t+1,s}) + m_s^{-1} \sum_{k \in N_s} \{\beta_{tk} - 0.5(\beta_{t-1,k} + \beta_{t+1,k})\}$. Hence, the conditional mean of β_{ts} depends on the latent process in region s at times $t-1$ and $t+1$, as well as the latent process in the spatial neighbors of region s at times $t-1$, t , and $t+1$. Thus, the first-order temporal trend evolution may be used for spatiotemporal smoothing. Therefore, this state-space specification may be useful after the epidemic ends its expansion phase and the disease becomes endemic.

The second state-space specification incorporates spatiotemporal contamination. Specifically, evolution with contamination assumes $\mathbf{F}'_t = \mathbf{I}_S$, and a contamination matrix $\mathbf{G}_t = (1 + \kappa h)^{-1} \mathbf{H}$, with $\{\mathbf{H}\}_{kl} = 1$ for $k = l$, $\{\mathbf{H}\}_{kl} = \kappa$ for $k \in C_l$, and $\{\mathbf{H}\}_{kl} = 0$ otherwise. Here, C_l is the set of across-time neighbors of subregion l , $h = \max_k \mathbf{1}(k \in C_l)$ is the maximum number of across-time neighbors, and $\kappa > 0$ is a contamination coefficient. Note that for full generality the set of across-time neighbors C_l may differ from the set of time-specific neighbors N_l . This contamination specification allows for abnormal increases at a given time point to spill over to neighboring regions at subsequent time points. Thus, we expect this contamination state-space specification to be useful during the initial periods of a disease emerging in a previously unaffected region.

The third state-space specification assumes a second-order temporal trend. The second-order temporal trend model assumes that $\boldsymbol{\beta}_t$ is comprised of two latent fields at time t , $\boldsymbol{\beta}_{1t} = (\beta_{1t1}, \dots, \beta_{1tS})'$ and $\boldsymbol{\beta}_{2t} = (\beta_{2t1}, \dots, \beta_{2tS})'$. Hence, this model assumes $\boldsymbol{\beta}_t = (\boldsymbol{\beta}'_{1t}, \boldsymbol{\beta}'_{2t})'$. In this specification, $\boldsymbol{\beta}_{1t}$ is equal to $\boldsymbol{\theta}_t$, the log-risk random field at time t . Furthermore, $\boldsymbol{\beta}_{2t}$ is the gradient field, that is, the expected increase in the log-risk random field from time t to time $t+1$. Specifically, the second-order temporal trend model assumes $\mathbf{F}'_t = (\mathbf{I}_S, \mathbf{0}_{SS})$, and evolution matrix

$$\mathbf{G}_t = \begin{pmatrix} \mathbf{G}_{1t} & \mathbf{G}_{1t} \\ \mathbf{0}_{SS} & \mathbf{G}_{2t} \end{pmatrix},$$

where $\mathbf{G}_{it} = \mathbf{I}_S$, $i = 1, 2$, and $\mathbf{0}_{SS}$ is an $S \times S$ matrix of zeros. Further, in the case of spatially correlated state-space innovations, we assume that \mathbf{W}_t^{-1} is block diagonal, that is, $\mathbf{W}_t^{-1} = \text{blockdiag}(\mathbf{W}_{1t}^{-1}, \mathbf{W}_{2t}^{-1})$, where $\mathbf{W}_{it}^{-1} = \tau_i(\mathbf{I}_S + \phi_i \mathbf{M})$, $i = 1, 2$. The second-order temporal trend model is appropriate when the temporal trend for each region can be approximated by a local linear trend that changes smoothly over time. Therefore, this model may be useful for describing the spatiotemporal evolution of the early stages of an emerging disease.

The fourth state-space specification assumes a field log-risk level and a common gradient for all counties at each time point. The common gradient at time t is a univariate parameter β_{2t} and evolves through time accordingly to the evolution equation $\beta_{2t} = \beta_{2,t-1} + \omega_{2t}$, where $\omega_{2t} \sim N(0, \psi^{-1})$ and ψ is the evolution precision for the common gradient. For this state-space specification, $\boldsymbol{\beta}_t = (\boldsymbol{\beta}'_{1t}, \beta_{2t})'$, $\mathbf{F}'_t = (\mathbf{I}_S, \mathbf{0}_S)$, and the evolution matrix is

$$\mathbf{G}_t = \begin{pmatrix} \mathbf{I}_S & \mathbf{1}_S \\ \mathbf{0}'_S & 1 \end{pmatrix},$$

where $\mathbf{0}_S$ and $\mathbf{1}_S$ are S -dimensional vectors of zeros and ones, respectively. For the fourth state-space specification, the state-space precision matrix is

$$\mathbf{W}_t^{-1} = \begin{pmatrix} \mathbf{W}_{1t}^{-1} & \mathbf{0}_S \\ \mathbf{0}'_S & \psi^{-1} \end{pmatrix}.$$

Finally, the fifth state-space specification assumes a contamination field model for the log-risk combined with a common gradient for all counties at each time point. Hence, almost all the components of the fifth state-space specification are the same as the components of the fourth state-space specification, except that the evolution matrix includes a contamination matrix and is given by

$$\mathbf{G}_t = \begin{pmatrix} (1 + \kappa h)^{-1} \mathbf{H} & \mathbf{1}_S \\ \mathbf{0}'_S & 1 \end{pmatrix},$$

where κ , h , and \mathbf{H} are defined as in the second state-space specification described above.

The models we describe above by no means exhaust the general class of models defined by Equations (1), (3), (4), and (5). In particular, many other models may be obtained as stochastic discretized versions of deterministic continuous time-space mathematical models. For example, these deterministic continuous time-space mathematical models may be based on partial differential equations and on integro-difference equations. For details on several possible deterministic continuous time-space mathematical models and how to discretize them, see Wikle and Hooten (2010) and references therein.

3 Bayesian Inference

This section develops simulation-based methods to perform full Bayesian statistical analysis for the class of spatiotemporal models defined by Equations (1), (3), (4), and (5). Specifically, we construct a Markov chain Monte Carlo (MCMC) algorithm (Gelfand and Smith, 1990; Robert and Casella, 2004; Gamerman and Lopes, 2006) to obtain samples from an approximate posterior distribution. Our computational methodology is general enough to be applied to observations with any distribution in the regular exponential family. However, here we focus on Poisson observations.

Let $\boldsymbol{\beta}_{0:T} = (\boldsymbol{\beta}'_0, \dots, \boldsymbol{\beta}'_T)'$ be the vectorized latent process collected through time, with similar notation for other quantities of the model. In addition, let $\boldsymbol{\psi}$ be the vector of unknown hyperparameters. Further, let \boldsymbol{D}_t , $t = 1, \dots, T$, represent all the information up to time t . Thus, \boldsymbol{D}_t is recursively defined as $\boldsymbol{D}_t = \boldsymbol{D}_{t-1} \cup \{\boldsymbol{y}_t\}$. Then, by Bayes Theorem the exact posterior density for $(\boldsymbol{\beta}_{0:T}, \boldsymbol{\psi})$ is proportional to

$$p(\boldsymbol{\beta}_{0:T}, \boldsymbol{\psi} | \boldsymbol{D}_T) \propto \left\{ \prod_{t=1}^T p(\boldsymbol{y}_t | \boldsymbol{\theta}_t, \boldsymbol{\eta}_t) \right\} \left\{ \prod_{t=1}^T p(\boldsymbol{\beta}_t | \boldsymbol{\beta}_{t-1}, \boldsymbol{\psi}) \right\} p(\boldsymbol{\beta}_0 | \boldsymbol{\psi}) p(\boldsymbol{\psi}).$$

The Markov chain used in our procedure has to be tailored to each specific spatiotemporal model and will depend on how the hyperparameter vector $\boldsymbol{\psi}$ appears in the matrices \boldsymbol{F}_t , \boldsymbol{G}_t and \boldsymbol{W}_t . However, the Markov chain may be partitioned in two blocks: simulation of $\boldsymbol{\psi}$,

which is model specific, and simulation of the latent process $(\boldsymbol{\beta}_0, \dots, \boldsymbol{\beta}_T)$. For the simulation of the latent process, we propose in Section 3.1 a novel extended forward filter backward sampler (EFFBS).

3.1 Extended Forward Filter Backward Sampler

This section introduces a novel extended forward filter backward sampler for the simulation of the latent process $(\boldsymbol{\beta}_0, \dots, \boldsymbol{\beta}_T)$. The EFFBS we propose combines the generalized extended Kalman filter (p. 352, Fahrmeir and Tutz, 2001) and the forward filter backward sampler method (FFBS) (Frühwirth-Schnatter, 1994; Carter and Kohn, 1994). Hence, the EFFBS is composed of two subsequent steps, that we describe below as the extended forward filter in Algorithm 3.1 and the backward sampler in Algorithm 3.2.

Let $\hat{\boldsymbol{\theta}}_t = (\hat{\theta}_{t1}, \dots, \hat{\theta}_{ts})'$ be a preliminary estimate of $\boldsymbol{\theta}_t$. This preliminary estimate may, for example, be the posterior mode obtained by the generalized extended Kalman filter. In addition, let $f'(\theta_{ts}) = n_{ts}e^{\theta_{ts}}$ denote the first derivative of the response function $f(\theta_{ts})$. Furthermore, let $\Sigma_{ts} = \text{Var}(y_{ts}) = n_{ts}e^{\theta_{ts}}$ be the variance of the number of disease cases at time t and region s . Then, the extended forward filter proceeds as follows.

Algorithm 3.1 (Extended forward filter) *Initiate the algorithm at time $t = 0$ with the distribution $\boldsymbol{\beta}_0 | \boldsymbol{\psi}, \mathbf{D}_0 \sim N(\mathbf{m}_0, \mathbf{C}_0)$. Then, for $t = 1, \dots, T$, do:*

1. *Prior at t : $\boldsymbol{\beta}_t | \boldsymbol{\psi}, \mathbf{D}_{t-1} \sim N(\mathbf{a}_t, \mathbf{R}_t)$, with*

$$\begin{aligned} \mathbf{a}_t &= \mathbf{G}_t \mathbf{m}_{t-1}, \\ \mathbf{R}_t &= \mathbf{G}_t \mathbf{C}_{t-1} \mathbf{G}_t' + \mathbf{W}_t. \end{aligned}$$

2. *Based on the first-order Taylor expansion of the response function f around $\hat{\boldsymbol{\theta}}_t = \mathbf{F}_t' \mathbf{a}_t$, compute the artificial observation vector $\hat{\mathbf{y}}_t = (\hat{y}_{t1}, \dots, \hat{y}_{ts})$ with*

$$\hat{y}_{ts} = \left\{ f'(\hat{\theta}_{ts}) \right\}^{-1} \left\{ y_{ts} - f(\hat{\theta}_{ts}) \right\} + \hat{\theta}_{ts}, \quad (6)$$

and the approximate precision matrix

$$\widehat{\mathbf{V}}_t^{-1} = \text{diag} \left[\frac{\left\{ f'(\widehat{\theta}_{ts}) \right\}^2}{\widehat{\Sigma}_{ts}} \right]. \quad (7)$$

3. Posterior at t : $\beta_t | \psi, \mathbf{D}_t \sim N(\mathbf{m}_t, \mathbf{C}_t)$, with

$$\mathbf{C}_t = \left(\mathbf{R}_t^{-1} + \mathbf{F}_t \widehat{\mathbf{V}}_t^{-1} \mathbf{F}_t' \right)^{-1}, \quad (8)$$

$$\mathbf{m}_t = \mathbf{C}_t \left(\mathbf{F}_t \widehat{\mathbf{V}}_t^{-1} \widehat{\mathbf{y}}_t + \mathbf{R}_t^{-1} \mathbf{a}_t \right). \quad (9)$$

The extended forward filter is an approximate method to calculate the mean vectors and covariance matrices of the posterior distributions $p(\beta_t | \psi, \mathbf{D}_t)$, $t = 1, \dots, T$. At the end of the extended forward filter, we have an approximation for the posterior distribution of the latent process at the last time point T given all the available information as well as the hyperparameter vector ψ , that is, $p(\beta_T | \psi, \mathbf{D}_T)$. Then, the backward sampler proceeds as follows.

Algorithm 3.2 (Backward sampler) Sampling from $\beta_{1:T} | \psi, \mathbf{D}_t$:

1. Sample β_T^* from the distribution $N(\mathbf{m}_T, \mathbf{C}_T)$, obtained from the extended forward filter.
2. For $t = T - 1, \dots, 0$, sample backwards β_t^* from the conditional distribution $N(\mathbf{b}_t, \mathbf{B}_t)$, where

$$\mathbf{B}_t = \left(\mathbf{C}_t^{-1} + \mathbf{G}_{t+1}' \mathbf{W}_{t+1}^{-1} \mathbf{G}_{t+1} \right)^{-1}, \quad (10)$$

$$\mathbf{b}_t = \mathbf{B}_t \left(\mathbf{G}_{t+1}' \mathbf{W}_{t+1}^{-1} \beta_{t+1}^* + \mathbf{C}_t^{-1} \mathbf{m}_t \right). \quad (11)$$

The EFFBS assumes an approximate Gaussian observational equation with artificial observation vector defined in (6) and approximate precision matrix given by (7). This implies that the EFFBS implicitly assumes the approximate likelihood function

$$k(\mathbf{y}_{1:T} | \boldsymbol{\theta}_{1:T}, \psi) = \prod_{t=1}^T k(\mathbf{y}_t | \boldsymbol{\theta}_t, \psi), \quad (12)$$

where $k(\mathbf{y}_t|\boldsymbol{\theta}_t, \boldsymbol{\psi})$ is proportional to

$$\left(\prod_{s=1}^S \hat{\Sigma}_{ts}\right)^{-1/2} \exp \left[-0.5 \sum_{s=1}^S (n_{ts} e^{\hat{\theta}_{ts}})^{-1} \left\{ y_{ts} - n_{ts} e^{\hat{\theta}_{ts}} + n_{ts} e^{\hat{\theta}_{ts}} \left(\hat{\theta}_{ts} - (\mathbf{F}'_t \boldsymbol{\beta}_t)_s \right) \right\}^2 \right].$$

Therefore, the MCMC algorithm with the embedded EFFBS defines a Markov chain that converges to an approximate posterior distribution with density

$$k(\boldsymbol{\beta}_{0:T}, \boldsymbol{\psi} | \mathbf{D}_T) \propto \left\{ \prod_{t=1}^T k(\mathbf{y}_t | \boldsymbol{\theta}_t, \boldsymbol{\psi}) \right\} \left\{ \prod_{t=1}^T p(\boldsymbol{\beta}_t | \boldsymbol{\beta}_{t-1}, \boldsymbol{\psi}) \right\} p(\boldsymbol{\beta}_0 | \boldsymbol{\psi}) p(\boldsymbol{\psi}).$$

Finally, at the end of the MCMC algorithm we have a sample $(\boldsymbol{\psi}^{(1)}, \boldsymbol{\beta}_{0:T}^{(1)}), \dots, (\boldsymbol{\psi}^{(G)}, \boldsymbol{\beta}_{0:T}^{(G)})$ from this approximate posterior distribution.

3.2 Model Comparison

With the ability to fit several nonnested spatiotemporal models comes the need to compare those models. Note also that, when analyzing a particular dataset, each of the possible models corresponds to a distinct scientific hypothesis. As such, comparison of the different models becomes paramount for understanding the nature of the process underlying the observed data. For the comparison of the nonnested spatiotemporal models introduced in Section 2, we develop a conditional Bayes factor (p. 190, Ghosh et al., 2006) that uses the output of the MCMC algorithm for the approximate posterior distribution. As we discuss below, this conditional Bayes factor provides a model comparison criterion that is justified from a Bayesian decision-theoretic point of view (Berger, 1985).

Bayesian model selection is usually performed by comparing the posterior probabilities of the competing models. When the competing models have equal prior probabilities, their posterior probabilities are proportional to their respective predictive densities. A potential difficulty in Bayesian model selection is that these predictive densities will be sensitive to the specification of the prior distribution for the hyperparameter vector $\boldsymbol{\psi}$. To overcome this

difficulty, we use here a training sample approach (Frühwirth-Schnatter, 1995) of the first t^* time observations; this results in calibrated priors for the parameters of each model. Then, Monte Carlo integration is used to compute the predictive distribution under each model for the remaining $T - t^*$ time observations.

Suppose that there are Q competing spatiotemporal models denoted by M_1, \dots, M_Q . The q th model has observational density $p_q(\mathbf{y}_t | \boldsymbol{\beta}_t, \boldsymbol{\Psi})$ and evolution density $p_q(\boldsymbol{\beta}_t | \boldsymbol{\beta}_{t-1}, \boldsymbol{\Psi})$. Let $p_q(\boldsymbol{\beta}_{0:(t-1)}, \boldsymbol{\Psi} | \mathbf{D}_{t-1})$ denote the joint posterior distribution of $\boldsymbol{\Psi}$ and $\boldsymbol{\beta}_0, \dots, \boldsymbol{\beta}_{t-1}$ under the q th model given the information up to time $t - 1$. Note that the definitions of the hyperparameter vector $\boldsymbol{\Psi}$ and the latent vector $\boldsymbol{\beta}_t$ may be (and in general will be) different under each model, but this distinction is omitted here to keep the notation simple. Then, under model q the one-step ahead predictive density of \mathbf{y}_t given the information up to time $t - 1$ is

$$p_q(\mathbf{y}_t | \mathbf{D}_{t-1}) = \int p_q(\mathbf{y}_t | \boldsymbol{\beta}_t, \boldsymbol{\Psi}) p_q(\boldsymbol{\beta}_t | \boldsymbol{\beta}_{t-1}, \boldsymbol{\Psi}) \times p_q(\boldsymbol{\beta}_{0:(t-1)}, \boldsymbol{\Psi} | \mathbf{D}_{t-1}) d\boldsymbol{\beta}_{0:(t-1)} d\boldsymbol{\beta}_t d\boldsymbol{\Psi}. \quad (13)$$

We apply the simulation scheme outlined in Section 3 to obtain G posterior draws

$$\left[\left(\boldsymbol{\beta}_{0:(t-1)}^{(1)}, \boldsymbol{\Psi}^{(1)} \right), \left(\boldsymbol{\beta}_{0:(t-1)}^{(2)}, \boldsymbol{\Psi}^{(2)} \right), \dots, \left(\boldsymbol{\beta}_{0:(t-1)}^{(G)}, \boldsymbol{\Psi}^{(G)} \right) \right].$$

Next, for $g = 1, \dots, G$, we simulate $\boldsymbol{\beta}_t^{(g)}$ given $(\boldsymbol{\beta}_{0:(t-1)}^{(g)}, \boldsymbol{\Psi}^{(g)})$ from the evolution distribution with density $p_q(\boldsymbol{\beta}_t | \boldsymbol{\beta}_{0:(t-1)}^{(g)}, \boldsymbol{\Psi}^{(g)})$. This yields the posterior sample $[(\boldsymbol{\beta}_{0:t}^{(1)}, \boldsymbol{\Psi}^{(1)}), \dots, (\boldsymbol{\beta}_{0:t}^{(G)}, \boldsymbol{\Psi}^{(G)})]$.

Now rewrite Equation (13) as

$$p_q(\mathbf{y}_t | \mathbf{D}_{t-1}) = \int p_q(\mathbf{y}_t | \boldsymbol{\beta}_t, \boldsymbol{\Psi}) p_q(\boldsymbol{\beta}_{0:t}, \boldsymbol{\Psi} | \mathbf{D}_{t-1}) d\boldsymbol{\beta}_{0:t} d\boldsymbol{\Psi}. \quad (14)$$

Equation (14) shows that $p_q(\mathbf{y}_t | \mathbf{D}_{t-1})$ is the expectation of $p_q(\mathbf{y}_t | \boldsymbol{\beta}_t, \boldsymbol{\Psi})$ with respect to $p_q(\boldsymbol{\beta}_{0:t}, \boldsymbol{\Psi} | \mathbf{D}_{t-1})$. Therefore, we can estimate the one-step ahead predictive density $p_q(\mathbf{y}_t | \mathbf{D}_{t-1})$ with

$$\hat{p}_q(\mathbf{y}_t | \mathbf{D}_{t-1}) = \frac{1}{G} \sum_{g=1}^G p_q(\mathbf{y}_t | \boldsymbol{\beta}_t^{(g)}, \boldsymbol{\Psi}^{(g)}). \quad (15)$$

Using the fact that the joint predictive density of $\mathbf{y}_{t^*+1}, \dots, \mathbf{y}_T$ can be written as $p_q(\mathbf{y}_{t^*+1}, \dots, \mathbf{y}_T | \mathbf{D}_{t^*}) = \prod_{t=t^*+1}^T p_q(\mathbf{y}_t | \mathbf{D}_{t-1})$, and as $\mathbf{D}_t = \mathbf{D}_{t-1} \cup \{\mathbf{y}_t\}$, an estimate of the joint predictive density under model q is (Vivar and Ferreira, 2009)

$$\hat{p}_q(\mathbf{y}_{t^*+1}, \dots, \mathbf{y}_T | \mathbf{D}_{t^*}) = \prod_{t=t^*+1}^T \hat{p}_q(\mathbf{y}_t | \mathbf{D}_{t-1}), \quad (16)$$

where t^* is such that $p_q(\boldsymbol{\psi} | \mathbf{D}_{t^*})$ is proper for all $q = 1, \dots, Q$. For a detailed discussion on the choice of t^* , see Vivar and Ferreira (2009). Then, based on the joint predictive density (16), for each pair of models we compute the conditional Bayes factor of model m against model n as

$$B_{mn} = \frac{\hat{p}_m(\mathbf{y}_{t^*+1}, \dots, \mathbf{y}_T | \mathbf{D}_{t^*})}{\hat{p}_n(\mathbf{y}_{t^*+1}, \dots, \mathbf{y}_T | \mathbf{D}_{t^*})}.$$

Finally, we use the conditional Bayes factors to decide what is the best model. In addition to being well justified theoretically, these conditional Bayes factors favor models that provide better probabilistic predictions.

4 Application

We illustrate the utility and flexibility of our Poisson spatiotemporal framework with an application to the number of acquired immunodeficiency syndrome (AIDS) cases in Rio de Janeiro State, Brazil. Specifically, we consider the annual number of new cases of AIDS from 1982 to 2007 for each of the 92 counties in Rio de Janeiro State. Data on the annual number of new cases of AIDS and on population size are publicly available from the Ministry of Health of Brazil and may be downloaded from the webpage www.datasus.saude.gov.br. From 1982 to 2007 new counties were created in Rio de Janeiro State. The data available on www.datasus.saude.gov.br about the number of new cases already use the geopolitical organization of Rio de Janeiro State as of 2007. However, data on population sizes are available for each year based on the geopolitical organization for each specific year. We have performed backcasting to obtain estimates of annual population sizes per county using the

geopolitical organization of Rio de Janeiro State as of 2007. The analysis that we present below is conditional on these county population sizes estimates.

AIDS is caused by the immunodeficiency virus (HIV), which has a long incubation period with a median of about 10 years in young adults (Bacchetti and Moss, 1989). Because the incubation period is much longer than the observational time unit of one year, we may expect the observed number of cases in one year to be a convolution of infections that have occurred in several previous years. As a result, the change from year to year in the underlying risk of observing new cases may exhibit a strong spatial dependence. This spatial dependence is accounted for in our modeling framework through the system equation innovation ω_t and its covariance matrix \mathbf{W}_t . Finally, given the time scale of the incubation period of about one decade and the fact that AIDS has emerged among humans about four decades ago, the AIDS epidemic provides an excellent case study of what may happen in terms of spatiotemporal dynamics when a previously unaffected region becomes infected by an emerging infectious disease.

We have implemented the Bayesian analysis procedures developed in Section 3 for each of the five spatiotemporal models described in Section 2.1. Specifically, we consider the following models with spatially dependent innovations: I – First-order field polynomial model; II – Contamination field model; III - Second-order field polynomial model; IV - Model with a field log-risk level and a common gradient for all counties at each time point; V - Contamination field model for the log-risk combined with a common gradient for all counties at each time point. Further, we have considered for each of these five models two specifications for the system equation innovations: spatial dependence, and spatial independence.

A Bayesian analysis requires the specification of priors both for the hyperparameters and for the latent process β_0 at time $t = 0$ given the information up to time 0 denoted by \mathbf{D}_0 . For the specification of the prior for β_0 for an emerging disease, we may use the information about the type of disease that we anticipate to observe. In the case of slowly progressing emerging epidemics such as in the case of AIDS in the beginning of the 1980s,

we expect the standardized risk for each county of the first case to appear at a given time to be about the reciprocal of the state population size. In the case of Rio de Janeiro State, the population size in 1981 ($t=0$) was about 11.5 million people. Hence, this corresponds to an expected logarithm of the risk equal to $E(\mathbf{F}'\boldsymbol{\beta}_0|\mathbf{D}_0) = \mathbf{1}_S \log(1/11,500,000) \approx -16.25 \mathbf{1}_S$. In addition, for an emerging disease we believe that the risk of the first case to appear at a given time to be within 20-fold of its expectation with probability 0.997. Further, we assume that before the disease emerges the standardized risk is stochastically independent between counties. These assumptions correspond in the logarithm scale to assuming $Var(\mathbf{F}'\boldsymbol{\beta}_0|\mathbf{D}_0) = \mathbf{I}_S$.

When assigning priors for the hyperparameters, we follow closely the recommendations of Vivar and Ferreira (2009). Specifically, we assume for the scale parameter τ_i a weakly informative *Gamma*(1, 1) prior; this prior imparts little information and concurrently guarantees posterior propriety. In addition, for the contamination coefficient κ we assume a noninformative uniform prior on the interval (0, 1). Further, for the spatial dependence parameter ϕ_i we assign a prior of the type $\Pi(\phi_i) \propto 1$ if $0 < \phi_i < 1$, $\Pi(\phi_i) \propto \phi_i^{-2}$ if $1 < \phi_i < a$, and $\Pi(\phi_i) \propto 0$ otherwise. See Vivar and Ferreira (2009) for an explanation on the relationship of this prior and the marginal reference prior for ϕ_i proposed by Ferreira and De Oliveira (2007) for PGMRFs. In particular, we have found that $a = 100$ works well in our current application.

Finally, for Models 4 and 5 that include a common gradient we assign a conditionally conjugate prior *Gamma*(a_ψ, b_ψ) for the log-gradient evolution precision ψ . First, to obtain a reasonably vague prior we assume $b_\psi = 0.1$ that implies the prior variance for ψ to be 10 times larger than the prior mean. Moreover, we expect the common gradient of the risk to be reasonably stable at subsequent time points. In particular, we expect the gradient to do not vary by much more than 20% between subsequent time points. This informs us that in the logarithm scale the evolution standard deviation $\psi^{-1/2}$ is probably less than 0.1; hence, we assign for this event a prior probability of about 0.95. This probability, together with

assuming $b_\psi = 0.1$ implies $a_\psi = 16$.

With respect to the MCMC algorithm, we ran two parallel chains, with distant initial starting points, for a total of 20,000 iterations for each chain, discarding the first 10,000 iterations for burn-in. Thus, inference was based on the last 10,000 iterations from each chain, for a total of 20,000 iterations. Convergence has been verified through the Gelman and Rubin convergence diagnostics (Gelman and Rubin, 1992), implemented in the CODA package of the R statistical software. Gelman and Rubin convergence diagnostics indicated convergence for each of the hyperparameters and for a sample of the latent process parameters.

We have applied the model selection approach developed in Section 3.2 to compare the five models. Here we use the first $t^* = 9$ time points as training sample for the computation of the conditional Bayes factors. Table 1 presents the conditional Bayes factors taking Model I as the baseline. A first feature that is clearly shown by the data is that, when compared with their spatially independent innovations counterparts, models with spatially dependent innovations (SDI) are better supported by the data. This supports the claim that the long incubation period of the HIV (Bacchetti and Moss, 1989) together with the annual frequency of the data would lead to spatially correlated field innovations. Thus, the data provide evidence of the usefulness of spatially dependent innovations to account for the fact that an increase in the risk of new cases of AIDS in a given year may reflect the convolution of HIV infections in several previous years.

Thus, we now focus on comparison of models with spatially dependent innovations. With a conditional Bayes factor equal to 84.7, the best is Model V that includes field contamination together with a common gradient for all counties. In addition, Model IV has a conditional Bayes factor somehow lower equal to 79.3. Model IV includes a first-order field level and a common gradient for all counties. Furthermore, Model III that is a second-order field model with a gradient field, that is a gradient for each county, has a very small Bayes factor equal to -1474.7. Thus, there is not enough information in the data to estimate a distinct gradient for each county. Therefore, the data provides evidence of the usefulness of the inclusion of

Table 1: AIDS Data - Logarithm of conditional Bayes factor (BF) (Baseline: Model I with spatially dependent innovations). SDI: spatially dependent innovations.

SDI	Model				
	I	II	III	IV	V
Yes	0	44.7	-1474.7	79.3	84.7
No	-3932.0	-1681.2	-2809.0	26.1	26.0

Table 2: Posterior summaries for the parameters of Model V that includes spatially dependent innovations with contamination field and a common gradient for all counties.

Parameter	Mean	95% Credible Interval
κ	0.001	(0.0005, 0.0014)
τ	7.16	(3.67, 11.92)
ϕ	0.50	(0.15, 1.14)
ψ	136.7	(79.2, 211.2)

both a contamination evolution for the log-risk level and a common gradient for all counties.

Table 2 provides posterior means and 95% credible intervals for the hyperparameters of the best model, Model V. A first feature that emerges from the table is that the contamination coefficient κ is most probably small with a posterior mean equal to 0.001 and a 95% credible interval given by (0.0005, 0.0014). Even though κ seems to be small, the logarithm of the conditional Bayes factor of Model V against the corresponding model without contamination, that is Model IV, is equal to $84.7 - 79.3 = 5.4$ and gives evidence in favor of including the contamination component in the model. Another feature that emerges is that ϕ , the parameter that controls the degree of spatial dependence of the innovations, is also small

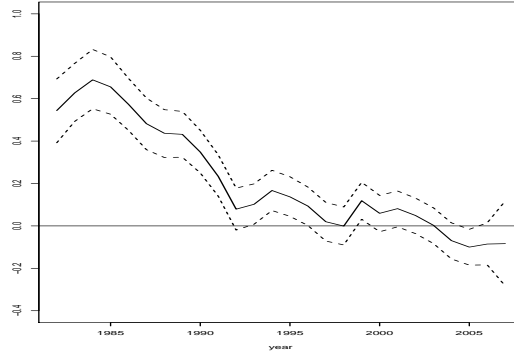


Figure 1: AIDS data - Common gradient for all counties for Model V. Posterior mean (solid line) and 95% credible interval (dashed lines).

with a posterior mean equal to 0.50 and a 95% credible interval given by (0.15, 1.14). This small value for ϕ has to be put in perspective by computing the conditional Bayes factor of Model V with spatially dependent against spatially independent innovations, that is equal to $84.7/26.0 = 58.7$. Hence, the data supports the hypothesis of spatially dependent innovations. Finally, the precision parameter ψ for the evolution of the common gradient has a posterior mean equal to 136.7 and a 95% credible interval given by (79.2, 211.2), implying that the common gradient evolves through time with small changes between subsequent time points.

Figure 1 presents the plot of common gradient of the log-risk level for all counties through time for Model V. Specifically, the figure presents the posterior mean (solid line) and 95% credible interval (dashed lines). This figure is quite informative, and clearly shows that there was a rapid expansion of the epidemic during the 1980's. Even though this rapid expansion was followed by a sharp reduction in the gradient in the beginning of the 1990's, the gradient continued to be small but mostly positive until about 2001. From 2003 to 2007 the gradient has been mostly negative, and fortunately the trend at the most recently considered year of 2007 was the reduction in the rate of new cases of AIDS.

Figure 2 shows for Model V the observed standardized ratio of new cases (left) and the

posterior mean of the risk (right) per 100,000 inhabitants for the years 1982, 1988, 1994, 2000 and 2006. The maps show the level of risk in a scale from white (low risk) to dark red (high risk). From a methodological perspective, our procedure accomplishes a nice balance between spatial and temporal smoothing resulting from the fact that Model V takes into account the information from spatial neighbors and from across-time neighbors. From an epidemiological perspective, two relevant features emerge from Figure 2. First, corroborating the findings from Figure 1, the rate of new cases increased substantially from the beginning of the 1980's to the end of the 1990's, and has somehow stabilized since 2000. Second, the rate of new cases is substantially higher in the metropolitan region of the City of Rio de Janeiro, located in the center-south of Rio de Janeiro State. These findings may be used by the Department of Health for allocating resources both for treatment and prevention of AIDS.

5 Conclusions

We have presented a novel class of spatiotemporal models for Poisson areal data that are useful for the statistical modeling of epidemics. Further, we have developed several specific models for count data with several distinct specifications of the evolution system equation to allow different spatiotemporal process behaviors with time-specific spatially correlated innovations. In addition, we have developed simulation-based full Bayesian analysis for both parameter estimation and model selection.

We have applied our spatiotemporal framework to analyze the number of new cases of AIDS per county in the State of Rio de Janeiro. Our spatiotemporal modeling framework has achieved a nice balance between spatial and temporal smoothing. In particular, it has become clear from our analysis that in the period of study the rate of new cases of AIDS was substantially higher in the metropolitan region of the City of Rio de Janeiro, and that in 2006 the rate of new cases seemed to be stabilizing. However, it is important to point out

that these were not good news, because the stabilization of the rate of new cases meant that the accumulated number of cases continued to increase over time.

From a modeling point of view, our general class of models may be tailored to specific applications. For example, when monitoring a particular disease, information on the natural history of the disease such as incubation time and rate of infection could potentially be incorporated in the spatiotemporal model. In one possible specification, parameters of the spatiotemporal model could be assumed to be functions of parameters of the natural history. In an alternative specification, the natural history parameters could be incorporated in the priors for the spatiotemporal model parameters. Finally, even though we have focused here on the analysis of Poisson data, our methodology is general enough to be applied to observations with any distribution in the regular exponential family. This may be useful for the analysis of spatiotemporal gamma-distributed survival data, and binomial-distributed survey data.

DISCLAIMER: Although Juan C. Vivar is an FDA/CTP employee, this work was not done as part of his official duties. This publication reflects the views of the authors and should not be construed to reflect the FDA/CTP’s views or policies.

References

- Anderson, R. M. and R. M. May (1992). *Infectious Diseases of Humans: Dynamics and Control*. New York: Oxford University Press.
- Apostolopoulos, Y. and S. Sönmez (2007). Demographic and epidemiological perspectives of human movement. In Y. Apostolopoulos and S. Sönmez (Eds.), *Population Mobility and Infectious Disease*, pp. 1–16. New York: Springer.
- Assuncao, R. M., I. A. Reis, and C. D. L. Oliveira (2001). Diffusion and prediction of leishmaniasis in a large metropolitan area in Brazil with a Bayesian space-time model. *Statistics in Medicine* 20, 2319–2335.

- Bacchetti, P. and A. R. Moss (1989). Incubation period of AIDS in San Francisco. *Nature* 338(6212), 251–253.
- Banerjee, S., B. P. Carlin, and A. E. Gelfand (2014). *Hierarchical Modeling and Analysis for Spatial Data*. Boca Raton: CRC Press.
- Berger, J. O. (1985). *Statistical Decision Theory and Bayesian Analysis, Second Ed.* New York: Springer.
- Bernardinelli, L., D. Clayton, C. Pascutto, C. Montomoli, M. Ghislandi, and M. Songini (1995). Bayesian analysis of space-time variation in disease risk. *Statistics in Medicine* 14, 2433–2443.
- Brower, J. and P. Chalk (2003). The global threat of new and reemerging infectious diseases: Reconciling U.S. national security and public health policy. Technical report, RAND Corporation, Santa Monica, CA.
- Carter, C. K. and R. Kohn (1994). On Gibbs sampling for state space models. *Biometrika* 81, 541–553.
- Casella, G. and R. L. Berger (2001). *Statistical Inference* (2nd ed.). Duxbury Press.
- Epstein, P. (2010). The ecology of climate change and infectious diseases: comment. *Ecology* 91(3), 925–928.
- Fahrmeir, L. and G. Tutz (2001). *Multivariate Statistical Modelling based on Generalized Linear Models* (2nd ed.). New York: Springer.
- Ferreira, M. A. R. and V. De Oliveira (2007). Bayesian reference analysis for Gaussian Markov Random Fields. *Journal of Multivariate Analysis* 98, 789–812.
- Frühwirth-Schnatter, S. (1994). Data augmentation and dynamic linear models. *Journal of Time Series Analysis* 15(2), 183–202.

- Frühwirth-Schnatter, S. (1995). Bayesian model discrimination and Bayes factors for linear Gaussian state-space models. *Journal of the Royal Statistical Society, Series B* 57, 237–246.
- Gamerman, D. and H. F. Lopes (2006). *Markov Chain Monte Carlo: Stochastic Simulation for Bayesian Inference* (2nd ed.). Boca Raton, FL: Chapman and Hall/CRC.
- Gelfand, A. E. and A. F. M. Smith (1990, June). Sampling-based approaches to calculating marginal densities. *Journal of the American Statistical Association* 85(410), 398–409.
- Gelman, A. and D. B. Rubin (1992). Inference from iterative simulation using multiple sequences. *Statistical Science* 7, 457–511.
- Ghosh, J. K., M. Delampady, and T. Samanta (2006). *An Introduction to Bayesian Analysis, Theory and Methods*. New York: Springer.
- Knorr-Held, L. (2000). Bayesian modelling of inseparable space-time variation in disease risk. *Statistics in Medicine* 19, 2555–2567.
- Lafferty, K. D. (2009). The ecology of climate change and infectious diseases. *Ecology* 90(4), 888–900.
- MacNab, Y. C. and C. B. Dean (2001). Autoregressive spatial smoothing and temporal spline smoothing for mapping rates. *Biometrics* 57, 949–956.
- McCullagh, P. and J. A. Nelder (1989). *Generalized Linear Models* (2nd. ed.), Volume 37 of *Monographs on Statistics and Applied Probability*. London: Chapman and Hall.
- Mugglin, A. S., N. Cressie, and I. Gemmell (2002). Hierarchical statistical modelling of influenza epidemic dynamics in space and time. *Statistics in Medicine* 21, 2703–2721.
- Prado, R., M. A. R. Ferreira, and M. West (2021). *Time Series: Modeling, Computation, and Inference* (2nd edition ed.). Boca Raton: CRC Press.

- Robert, C. P. and G. Casella (2004). *Monte Carlo Statistical Methods* (2nd ed.). Springer-Verlag.
- Schmid, V. and L. Held (2004). Bayesian extrapolation of space-time trends in cancer registry data. *Biometrics* *60*, 1034–1042.
- Sun, D., R. K. Tsutakawa, H. Kim, and Z. He (2000). Spatio-temporal interaction with disease mapping. *Statistics in Medicine* *19*, 2015–2035.
- Tzala, E. and N. Best (2008). Bayesian latent variable modelling of multivariate spatio-temporal variation in cancer mortality. *Statistical Methods in Medical Research* *17*, 97–118.
- Vivar, J. C. and M. A. R. Ferreira (2009). Spatio-temporal models for gaussian areal data. *Journal of Computational and Graphical Statistics* *18*, 658–674.
- Waller, L. A., B. P. Carlin, H. Xia, and A. E. Gelfand (1997). Hierarchical spatio-temporal mapping of disease rates. *Journal of the American Statistical Association* *92*, 607–617.
- West, M., P. J. Harrison, and H. S. Migon (1985). Dynamic generalized linear models and Bayesian forecasting (with discussion). *Journal of the American Statistical Association* *80*, 73–96.
- Wikle, C. K. and M. B. Hooten (2010). A general science-based framework for dynamical spatio-temporal models. *Test* *19*, 417–451.

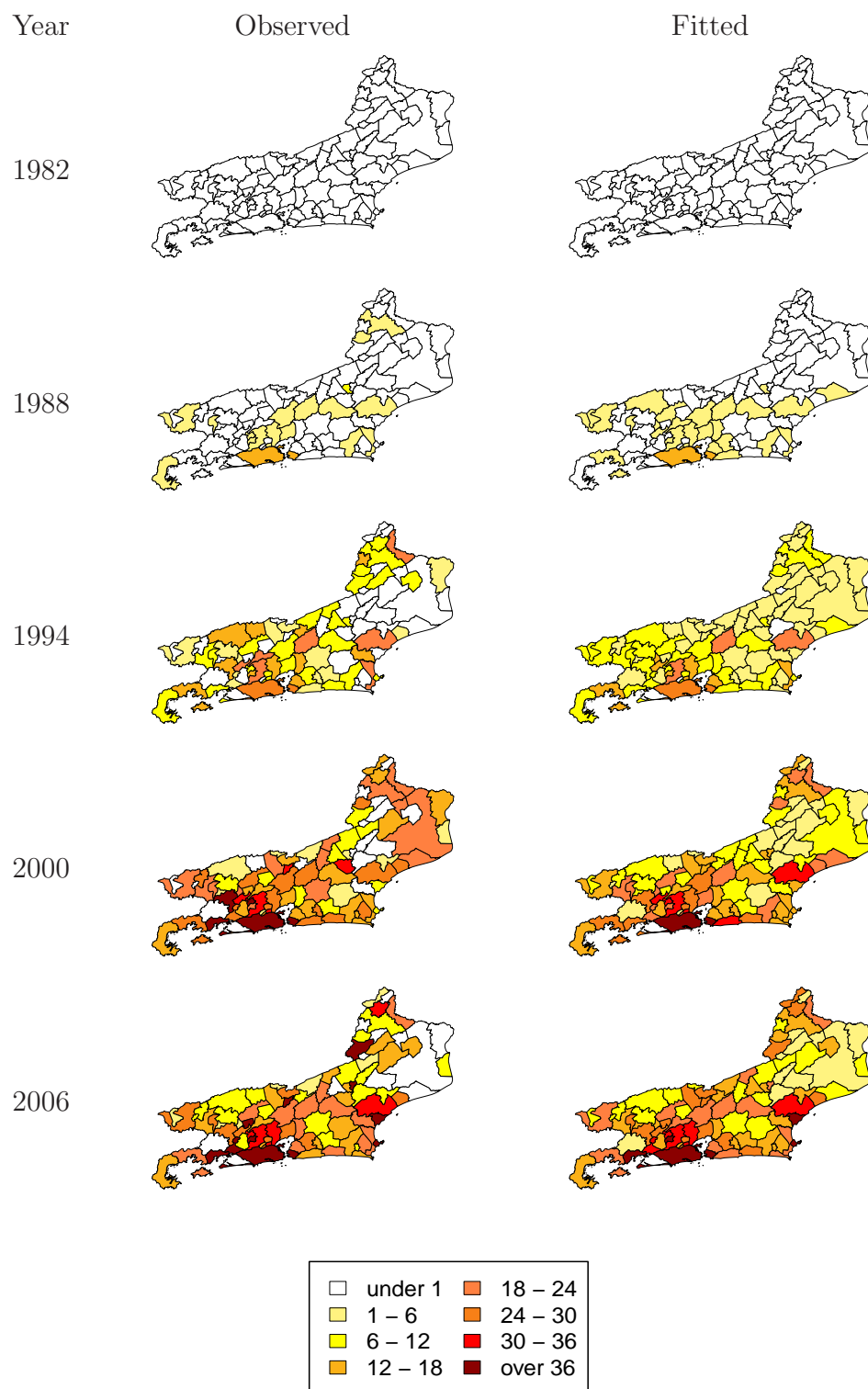


Figure 2: AIDS data - Model V. Standardized ratio of new cases per 100,000 inhabitants: observed (left panels), and fitted (right panels).